X-ray Absorption Spectroscopy Measurements of Liquid Water

L.-Å. Näslund,[†,‡] J. Lüning,[‡] Y. Ufuktepe,[‡,§] H. Ogasawara,[‡] Ph. Wernet,[‡,⊥] U. Bergmann,[‡] L. G. M. Pettersson,[†] and A. Nilsson*[,†,‡]

FYSIKUM, Stockholm University, Albanova University Center, S-106 91 Stockholm, Sweden, Stanford Synchrotron Radiation Laboratory, P.O. Box 4349, MS 69 Stanford, California 94309, and Physics Department, University of Cukurova, 01330 Adana, Turkey

Received: April 20, 2005; In Final Form: June 1, 2005

Recent studies, based on X-ray absorption spectroscopy (XAS) and X-ray Raman scattering (XRS), have shown that the hydrogen bond network in liquid water consists mainly of water molecules with only two strong hydrogen bonds. Since this result is controversial, it is important to demonstrate the reliability of the experimental data, which is the purpose of this paper. Here we compare X-ray absorption spectra of liquid water recorded with five very different techniques sensitive to the local environment of the absorbing molecule. Overall, the spectra obtained with photon detection show a very close similarity and even the observable minor differences can be understood. The comparison demonstrates that XAS and XRS can indeed be applied reliably to study the local bonding of the water molecule and thus to reveal the hydrogen bond situation in bulk water.

1. Introduction

Measuring the electronic structure to elucidate the nature of liquid water has been a challenge for many years. X-ray absorption spectroscopy (XAS), also known as near-edge X-ray absorption fine structure (NEXAFS) or X-ray absorption near-edge structure (XANES) spectroscopy, has proved to be a powerful technique for electronic structure studies. Its application requires advanced detection systems and intense X-ray sources with a continuous spectrum, which can be produced by, e.g., a third generation synchrotron facility.[1] In particular the ultrahigh vacuum (UHV) environment required at the synchrotron beamline has rendered oxygen *K*-edge (O 1s) XAS of water problematic due to the high vapor pressure of the liquid. To avoid this problem Yang and Kirz kept a thin liquid water film between two Si_3N_4-windows[2] and later Bowron et al.[3] presented a study where the absorption coefficient was obtained by X-ray Raman scattering (XRS) where a high-energy photon undergoes an energy-loss scattering event that corresponds to a core level excitation process.[4] Although these experiments demonstrated the feasibility of such measurements, no information about the hydrogen (H) bond structure in liquid water could be derived because of the only moderate spectral resolution achievable at that time.

Recently a series of investigations have demonstrated that XAS and XRS can reveal unique information about the structure of water in the bulk liquid phase,[5−7] at the liquid surface,[8,9] in ice,[10,11] at the ice surface,[9,10] and adsorbed as monolayers on metal surfaces.[12] In particular the interpretation of the bulk liquid spectra, which suggests a substantially smaller amount than expected of strong H bonds in liquid water, is controversial. The X-ray absorption (XA) spectrum of liquid water (see Figure 1) shows a strong preedge peak at 535.0 eV, a main-edge peak at 537.6 eV, and a postedge peak around 540.4 eV.[7] These features reflect the 2p character of the unoccupied valence orbitals at the site of the oxygen (O) atom of the water molecule. Through model experiments, i.e., tetrahedrally coordinated bulk ice and broken donating H-bond structures at the ice surface, as well as density functional theory (DFT) calculations of XA spectra for clusters of water molecules, the spectral features could be related to specific molecular environments. In particular, the weakly coordinated OH in molecules with asymmetric donating H bonds gives rise to the strong preedge feature observed for liquid water as well as for the ice surface, while the more strongly H-bonded OH contributes to the postedge peak.[5,7,13] The similarity of the ice surface and liquid water spectra and the comparison between the DFT calculated bond situations and experimental data suggest that liquid water consists mainly of water molecules with only one strong donating H bond (H bond on the hydrogen side), also denoted as single donor (SD) configuration.[7] The other donated H bond is "broken" or "weak" due to either elongation or bending of the OH- - -O axis[7] with a higher probability for bending in order to be consistent with radial distribution function (RDF) data obtained from neutron diffraction studies.[14] The investigation thus shows that a dominant fraction of water molecules are in configurations with only two strong H bonds, one donating and one accepting, with the configurations connected via a three-dimensional weakly H-bonded network.[7] This indicates a major discrepancy with molecular dynamics (MD) simulations, which suggest that most molecules are in local tetrahedral configurations not too different from ice.[7,15]

This picture was recently challenged in a study by Smith et al.,[16] who used XAS measurements with total electron yield (TEY) detection to obtain temperature-dependent spectra of a microjet of liquid water. Their claim that the tetrahedral model, as obtained by MD simulations, is consistent with the spectra based on a Boltzmann analysis of the temperature-dependent

* Address correspondence to this author. Phone: +1 (650) 926-2233. Fax: +1 (650) 926-4100. E-mail: nilsson@slac.stanford.edu.
† Stockholm University.
‡ Stanford Synchrotron Radiation Laboratory.
§ University of Cukurova.
⊥ Present address: BESSY, Albert-Einstein Strasse 15, D-12489 Berlin, Germany.

10.1021/jp052046q CCC: $30.25
Published on Web 06/25/2005

TABLE 1: Comparison of the Different Measurements of the Absorption Spectrum of Liquid Water with Distinctions in Terms of Detection Modes, X-ray Sources, Sample Conditions, Probing Depths, and Sample Temperatures[a]

spectrum	technique	X-ray source	sample conditions	probing depth	sample temp	ref
a	AEY	ALS BL 9.0	condensed droplet	2 nm	−2 °C	18
b	TEY	ALS BL 8.0	20 μm microjet	? nm	ca. 10 °C	19
c	T mode.	SSRL BL 10	steady water between Si_3N_4-windows	400 nm	room temp	this work
d	XRS	APS BL 18-D	flowing water in tube	150 μm	room temp	20
e	FY	ALS BL 8.0	steady water in straw	300 nm	room temp	21

[a] The detection modes refer to Auger-electron yield (AEY), total electron yield (TEY), transmission mode (T mode), X-ray Raman scattering (XRS), and fluorescence yield (FY). For the X-ray sources the abbreviations of the names of the synchrotron facilities and the names of the beamlines (BL) are given: Advanced Light Source (ALS), Berkeley, USA; Stanford Synchrotron Radiation Laboratory (SSRL), Menlo Park, USA; and Advanced Photon Source (APS), Argonne, USA. Further details of the experimental setups and sample preparations can be found in the references in the rightmost column.

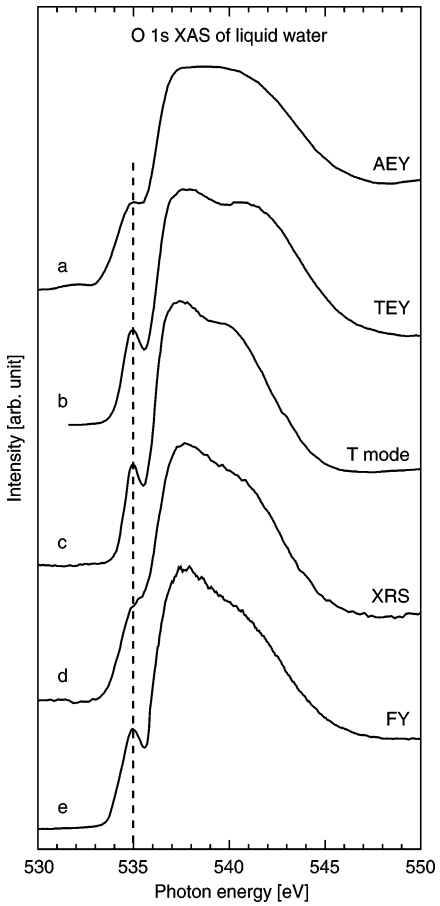

Figure 1. O K-edge X-ray absorption spectra of liquid water, recorded by (a) Auger-electron yield (AEY) XAS (taken from ref 9), (b) total electron yield (TEY) XAS (taken from ref 16), (c) transmission mode (T mode) XAS, (d) X-ray Raman scattering (XRS) (taken from ref 7), and (e) fluorescence yield (FY) XAS corrected for saturation effects as described in detail in ref 21. All spectra are normalized by area between 532 and 550 eV and shifted to line up the preedge feature at 535.0 eV (dotted line) for impartial comparison. The experimental resolution is 0.1 eV for the XAS spectra and ~1 eV for the XRS spectrum.

variation of spectral features. An energy difference between species which would be consistent with the energy cost for small geometry distortions seen in MD simulations was derived. It was later demonstrated that both the measurement and analysis in Smith et al. suffered from serious shortcomings due to experimental artifacts and incorrect assumptions about spectral profiles for the Boltzmann analysis.[17] The discrepancy with MD simulations thus remains.

Given this discrepancy it is important to scrutinize the experimental data and quantitatively evaluate the reliability of XAS/XRS measurements. In this paper various XA spectra of liquid water recently presented in the literature are compared with a newly recorded transmission mode (T mode) XA spectrum. Different experimental approaches have been used for the spectra discussed here but, despite variations in sample preparation and different detection modes, our analysis shows that the spectra obtained with photon detection are very similar and provide a consistent picture of the liquid.

2. Experimental Section

Several ways to record XA spectra with high spectral resolution are available today. In addition to transmission XAS and XRS one can also measure XA spectra indirectly via secondary yield techniques. Instead of measuring the X-ray absorption at the O *K*-edge directly in transmission mode the secondary yield techniques use secondary processes where the generated core hole decays via either radiative or nonradiative processes.[1] The radiative detection scheme is often denoted fluorescence yield (FY) while the nonradiative mode can be divided into Auger-electron yield (AEY) and total electron yield (TEY) detection. In the nonradiative process the core hole decays via the Auger process, giving rise to a high kinetic energy Auger electron that is detected via an energy dispersive electron analyzer to yield the AEY signal. The majority of the Auger electrons are, however, scattered within the material, which gives rise to a scattering cascade of low kinetic energy electrons. Monitoring all electrons escaping the surface yields the TEY signal.

The experimental conditions for the different XA spectra discussed here are summarized in Table 1. Details of the experimental setups can be found elsewhere[18−21] except for the T mode measurements. To record T mode spectra, thin water films were prepared by squeezing a water droplet between two Si_3N_4 membranes. Thicknesses from about 300 to 500 nm were prepared by adding polystyrene nanospheres of corresponding size[22] to the water droplets (about 1 vol %). A contribution of the added nanospheres to the observed oxygen XA spectra can be excluded, since samples with very different nanosphere concentrations yielded identical spectra. The film thicknesses were determined by comparison of measured and calculated transmission intensities at nonresonant photon energies for which tabulated values are available.[23] To preserve the thin films from drying out, the sample holders were sealed around the edges of the Si wafers carrying the Si_3N_4 membranes. These sandwiched films were then put into the experimental chamber, which was backfilled with He at atmospheric pressure. Photon energy scans were recorded with and without the sample in the X-ray beam, using a photodiode placed behind the sample. The ratio of these two measurements gives the transmission spectrum. To correct for intensity variations in the incoming X-ray beam an I_0 monitor within the UHV section of the beamline was used. This gave very reliable experimental data as verified by repeated scans

over extended periods of time. Since the X-rays penetrate the entire water film, spectra recorded in transmission mode are inherently bulk sensitive. The measurements were performed at the Stanford Synchrotron Radiation Laboratory (SSRL) on beamline 10-1 with a spectral resolution of better than 150 meV.

There are several different methods to energy calibrate an XA spectrum, which are also often unique for the selected technique. Small deviations in the absolute energy scale may therefore occur. The energy calibration procedure applied in the FY XAS measurement involves a reference structure in the recorded XA spectrum due to gas-phase water.[21] The third gas-phase peak, the O1s transition into the first Rydberg orbital, is sharp and easily detectable. Knowing its energy position of 537.25 eV[21] the spectrum can be shifted to the correct energy. For easier comparison in the following discussion of XA spectra of liquid water obtained with different techniques, all spectra are shifted to line up the preedge feature at 535.0 eV as obtained in the thus energy calibrated FY XA spectrum.

3. Results and Discussion

Figure 1 presents XA spectra of liquid water recorded with different techniques. The overall similarity of these spectra in terms of the different spectral features is immediately apparent. Note that the XRS spectrum was taken with about 1 eV experimental resolution, whereas the energy resolution in the other cases was substantially higher such that limitations in resolution do not significantly contribute to the width of the observed structures. However, there are some differences in spectral width and relative intensities between spectra obtained with electron detection and the other methods. In the following we will present a detailed comparison of these spectra and discuss the observable differences and their possible origin.

The fluorescence yield spectrum has been corrected for saturation effects, which can occur if the sampling depth is not significantly smaller than the X-ray penetration length. This can result in compressed spectral features and saturation of the XA spectrum. The standard procedure applied to correct the FY spectrum is:

$$\mu_x(h\nu) = C'(\epsilon_f)\frac{I_f(h\nu)}{I_0}\Big/\left(1 - C''(\epsilon_f)\frac{I_f(h\nu)}{I_0}\right)$$

where μ_x is the desired linear absorption coefficient, I_f is the fluorescence yield signal, I_0 is the incident photon flux density, $C'(\epsilon_f)$ is a scaling factor, and $C''(\epsilon_f)$ is the saturation compensating factor for the fluorescence with energy ϵ_f. Further details are described elsewhere.[21,24]

In the two electron yield spectra (AEY and TEY) the main absorption resonance (536−546 eV) appears to be broader. Electron detection is often used for its high detection efficiency.[1] A key feature of electron detection is the short mean free path of electrons in matter, which may make the electron detection surface or near-surface sensitive. This is in particular the case for the AEY spectrum where the requirement that the registered electrons have not undergone any inelastic scattering processes implies a short mean free path of around 2 nm.[25,26] While this is advantageous in many applications, it causes AEY spectra of liquid water to actually map the H bond structure only in the near-surface region, which does not necessarily correspond to the bulk structure. In fact, the AEY spectrum shows a more pronounced postedge peak, which is furthermore shifted toward higher energies as indicated by the larger width of the spectrum. The intensity at the postedge is attributed to coordinated OH groups, i.e., either the strongly H-bonded OH group in SD species or to double-donor (DD) species with both OH groups H bonded as in, e.g., tetrahedrally coordinated water. The peak position of the postedge is furthermore sensitive to the distance between the two oxygen atoms in the H bond with the peak moving to higher energy for shorter distances following the concept of "bond length with the ruler".[1,27] The AEY spectrum thus indicates that the near-surface region contains water molecules not only with more H-bonded OH groups, but also with slightly shorter H-bonding distances compared to bulk water. This is actually in contradiction to the results of an EXAFS study by Wilson et al.[28] reporting a 5.9% expansion of the O−O distances in the liquid surface region. It is clear that the presence of the water surface seems to give a structure that is different from the bulk and we therefore expect differences in the spectral shape.

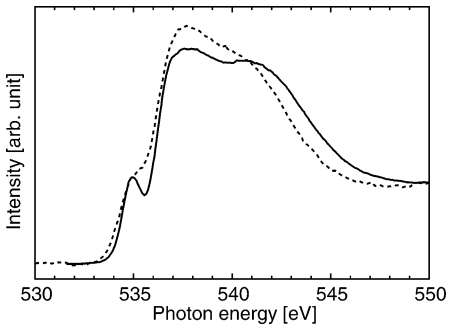

Figure 2. Comparison between the TEY XAS spectrum[16] (solid) and XRS spectrum[7] (dotted) measured at 288 and 298 K, respectively. Both spectra are normalized by area between 532 and 550 eV for impartial comparison. The main differences between the spectra are that the TEY XAS spectrum has a lower maximum intensity at the main-edge peak and a broader continuum, which are characteristic symptoms of saturation effects. The difference in temperature of 10 K between the two measurements is small enough to not have any significant effect on the spectral profile.[7,17]

Low-energy electrons that have undergone many inelastic scattering events dominate the electron signal monitored in TEY, which therefore samples deeper into the liquid bulk. The Auger-electron cascade process following the primary photoabsorption involves many inelastic scattering events leading to a large detection depth for absorption events registered through low-energy electrons. In the first step a core hole is generated that subsequently decays by Auger-electron emission with kinetic electron energies around 500 eV. The Auger electrons undergo inelastic scattering processes that lower the electron kinetic energy. It has been determined in theoretical simulations of the Auger-electron cascade process in water that each Auger electron gives rise to 20 secondary electrons with many inelastic scattering events.[29]

Figure 2 shows a detailed comparison between the TEY and XRS spectra. We can note important differences: the TEY is clearly much broader and the maximum intensity is much lower. This is often observed when XA spectra suffer from the saturation effect.[30] In this case it is not trivial to make a correction as in FY saturation since the mean free path of the electrons is not known.

Although qualitatively all five detection modes give similar spectra, it is clear that the observable differences would, in a quantitative analysis, lead to slightly different results. Since surface effects (AEY) and saturation effects (TEY) are likely to affect the spectra of the electron yield techniques we will focus in the remaining discussion on the spectra obtained with the inherently bulk sensitive photon detection techniques. A comparison between the T mode, XRS, and FY spectra (highlighted in Figure 3) shows only minor differences. Since

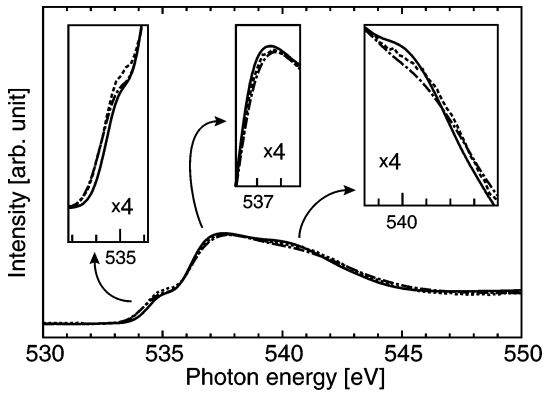

Figure 3. Comparison between the T mode XAS spectrum (solid), XRS spectrum (dotted), and FY XAS spectrum (dash−dotted), where the two XAS spectra are convoluted to give the same resolution as the XRS spectrum.[31] All spectra are normalized by area between 532 and 550 eV for impartial comparison. The insets highlight the main differences.

the XRS spectrum has been recorded with significantly lower spectral resolution, the T mode and the FY spectra have been convoluted with a Gaussian to reflect equivalent spectral resolution.[31] The main differences are that the intensity of the preedge peak at 535 eV is higher in the XRS spectrum and that the preedge peak seems to be sharper for the T mode spectrum. The T mode spectrum also has slightly larger intensity at the main-edge peak. At the postedge peak around 540 eV the T mode spectrum has a higher intensity than the XRS and the FY spectra, where the latter has the lowest postedge peak intensity.

The higher relative intensity of the postedge peak in the T mode spectrum could be interpreted as that the T mode spectrum has more contribution of tetrahedrally coordinated species than the other two. It could be possible that there are structural rearrangements of liquid water near the Si_3N_4-windows and around the added polystyrene nanospheres causing interface effects. It has been proposed that a 1 nm thick region of 4-fold coordinated water is present near an interface in confined spaces.[32−37] Assuming that the T mode spectrum probes a 400 nm thick water film, the contribution of such 4-fold coordinated molecules to the measured spectrum should be less than 1%, which is unlikely to cause such a comparatively large effect as shown in Figure 3. The more pronounced postedge feature may thus indicate that this ordered layer extends further than expected into the bulk of the water film. The confinement of the water film may also be the reason the preedge peak is sharper in the T mode spectrum. The XRS technique, which also uses a cell to hold the sample with a window for the X-rays,[6,7] has a detection depth of $\sim$150 μm.[38] Hence it is unlikely that an ordered layer at the window surface should have any noticeable effect on the XRS spectra.

The differences in the relative preedge intensity of the XRS spectrum as compared to the T mode spectrum and the FY spectrum (Figure 3) could in principle be caused by small contributions of nondipole transitions due to momentum (q) transfer in the XRS process. However, the spectrum shown here was taken at $q = 3$ Å^{-1} and no significant changes have been observed between data taken at $q = 3$ and 4 Å^{-1} indicating that the nondipole effects are reduced to a minimum.[39] The XRS spectrum may, however, still have some minor contributions from nondipole transitions but this small amount does not affect the interpretation of the liquid water spectrum.

One possible source of uncertainty arises from the fact that the three photon detection based measurements are accomplished at three different synchrotron facilities, see Table 1. The performance of the beamline monochromator may give some deviation in energy, I_0 structures due to energy-dependent reflectivities of the beamline optics may be difficult to normalize out properly, higher order reflections may affect the recorded spectrum, and detector response can vary with photon energy.[1] These examples are well-known sources of artifacts and special care to minimize the effects is included in the preparation procedure (beamline tuneup and experimental setup adjustments) before recording the spectra. In the case of the three spectra in Figure 3 there may be contributions of artifacts originating from actual beamlines, but rigorous controls have kept these contributions at a small level.

The differences between the T mode, FY, and XRS spectra are thus small and the three different techniques investigated give a very consistent picture of the electronic structure of the liquid. This excludes uncertainties in the experimental data as a source for the discrepancies with MD simulations in the understanding of the structure of liquid water.

4. Conclusions

In summary we note that transmission XAS is the most direct way to record an absorption spectrum. However, the required small film thickness makes the sample preparation difficult and complicates manipulation of the liquid sample during the experiment. Nevertheless, as shown here, it can be applied to obtain a reliable high-resolution absorption spectrum of the bulk of a thin water film. The most reliable technique to measure the absorption spectrum of ambient liquid water is XRS with small momentum transfer ($q < 3$ Å^{-1}). The drawback is the present limited spectral resolution when using hard X-ray beamlines and current X-ray spectrometers. The challenge of the XRS technique is to obtain better energy resolution with sufficient sensitivity. Cai et al.[11] have obtained water XRS spectra with <0.2 eV resolution; however, their sensitivity was still very low ($\sim$1 count/s). New efficient multicrystal high-resolution devices currently under construction will overcome this difficulty by combining high efficiency with good energy resolution. In the meantime XAS measured with the FY technique provides well-resolved spectral features of bulk water where, however, the spectra may need to be corrected for saturation effects by, e.g., comparing the intensities with the inherently saturation free XRS spectrum. We conclude that all three bulk-sensitive techniques (fluorescence yield XAS, transmission XAS, and XRS) give very similar and consistent spectra reflecting the H-bonding structure in bulk liquid water. However, it is important to be careful in the usage of electron detection to probe bulk water with XAS since there can be a large variation in the detection depth depending on the kinetic energy of the detected electrons. This can result in either surface effects (AEY) or saturation effects (TEY) which are difficult to correct due to large variations of the electron mean free paths for electrons with different kinetic energy.

Acknowledgment. This work was supported by the Swedish Foundation for Strategic Research, Swedish Natural Science Research Council, and National Science Foundation (U.S.) grants CHE-0089215 and CHE-0431425. The Advanced Light Source is supported by the Director, Office of Science, Office of Basic Energy Sciences, Material Sciences Division, of the U.S. Department of Energy under Contract No. DE-AC03-76SF00098 at Lawrence Berkeley National Laboratory. Portions of this research were carried out at the Stanford Synchrotron Radiation Laboratory, a national user facility operated by Stanford University on behalf of the U.S. Department of Energy,

Office of Basic Energy Sciences. Use of the Advanced Photon Source was supported by the U.S. Department of Energy, Basic Energy Sciences, Office of Science, under contract No. W-31-109-ENG-38. BioCAT is a National Institutes of Health-supported Research Center RR-08630. Y.U. acknowledges support by the Department of Energy Cooperative Research Program for the SESAME project.

References and Notes

(1) Stöhr, J. *NEXAFS Spectroscopy*; Springer-Verlag: New York 1992.

(2) Yang, B. X.; Kirz, J. *Phys. Rev. B* **1987**, *36*, 1361.

(3) Bowron, D. T.; Krisch, M. H.; Barnes, A. C.; Finney, J. L.; Kaprola, A.; Lorenzen, M. *Phys. Rev. B* **2000**, *62*, R9223.

(4) Mizuno, Y.; Ohmura, Y. *J. Phys. Soc. Jpn.* **1967**, 22, 445.

(5) Myneni, S.; Luo, Y.; Näslund, L-Å.; Cavalleri, M.; Ojamäe, L.; Ogasawara, H.; Pelmenschikov, A.; Wernet, Ph.; Väterlein, P.; Heske, C.; Hussain, Z.; Pettersson, L. G. M.; Nilsson, A. *J. Phys.*: *Condens. Matter* **2002**, *14*, L213.

(6) Bergmann, U.; Wernet, Ph.; Glatzel, P.; Cavalleri, M.; Pettersson, L. G. M.; Nilsson, A.; Cramer, S. P. *Phys. Rev. B* **2002**, *66*, 092107.

(7) Wernet, Ph.; Nordlund, D.; Bergmann, U.; Cavalleri, M.; Odelius, M.; Ogasawara, H.; Näslund, L.-Å.; Hirsch, T. K.; Ojamäe, L.; Glatzel, P.; Pettersson, L. G. M.; Nilsson, A. *Science* **2004**, *304*, 995.

(8) Wilson, K. R.; Cavalleri, M.; Rude, B. S.; Schaller, R. D.; Nilsson, A.; Pettersson, L. G. M.; Goldman, N.; Catalano, T.; Bozek, J. D.; Saykally, R. J. *J. Phys.*: *Condens. Matter* **2002**, *14*, L221.

(9) Bluhm, H.; Ogletree, D. F.; Fadley, C. S.; Hussain, Z.; Salmeron, M. *J. Phys.*: *Condens. Matter* **2002**, *14*, L227.

(10) Nordlund, D.; Ogasawara, H.; Wernet, Ph.; Nyberg, M.; Odelius, M.; Pettersson, L. G. M.; Nilsson, A. *Chem. Phys. Lett.* **2004**, *395*, 161.

(11) Cai, Y. Q.; Mao, H. K.; Chow, P. C.; Tse, J. S.; Ma, Y.; Patchkovskii, S.; Shu, J. F.; Struzhkin, V.; Hemley, R. J.; Ishii, H.; Chen, C. C.; Jarrige, I.; Chen, C. T.; Shieh, S. R.; Huang, E. P.; Kao, C. C. *Phys. Rev. Lett.* **2005**, *94*, 025502.

(12) Ogasawara, H.; Brena, B.; Nordlund, D.; Nyberg, M.; Pelmenschikov, A.; Pettersson, L. G. M.; Nilsson, A. *Phys. Rev. Lett.* **2002**, *89*, 276102.

(13) Cavalleri, M.; Ogasawara, H.; Pettersson, L. G. M.; Nilsson, A. *Chem. Phys. Lett.* **2002**, *364*, 363.

(14) Soper, A. K. *Chem. Phys.* **2000**, *258*, 121.

(15) Luzar, A.; Chandler, D. *Phys. Rev. Lett.* **1996**, *76*, 928.

(16) Smith, J. D.; Cappa, C. D.; Wilson, K. R.; Messer, B. M.; Cohen, R. C.; Saykally, R. J. *Science* **2004**, *306*, 851.

(17) Nilsson, A.; Wernet, Ph.; Nordlund, D.; Bergmann, U.; Cavalleri, M.; Odelius, M.; Ogasawara, H.; Näslund, L.-Å.; Hirsch, T. K.; Ojamäe, L.; Glatzel, P.; Pettersson, L. G. M. *Science* **2005**, *308*, 793.

(18) Ogletree, D. F.; Bluhm, H.; Lebedev, G.; Fadley, C. S.; Hussain, Z.; Salmeron, M. *Rev. Sci. Instrum.* **2002**, *73*, 3872.

(19) Wilson, K. R.; Rude, B. S.; Smith, J.; Cappa, C.; Co, D. T.; Schaller, R. D.; Larsson, M.; Catalano, T.; Saykally, R. J. *Rev. Sci. Instrum.* **2004**, *75*, 725.

(20) Bergmann, U.; Glatzel, P.; Cramer, S. P. *Microchem. J.* **2002**, *71*, 221.

(21) Näslund, L.-Å.; Edwards, D. C.; Wernet, Ph.; Bergmann, U.; Ogasawara, H.; Pettersson, L. G. M.; Myneni, S.; Nilsson, A. *J. Phys. Chem. A* **2005**, in press.

(22) Polystyrene nanospheres with very small size distributions were obtained from Duke Scientific Corporation, www.dukescientific.com.

(23) Henke, B. L.; Gullikson, E. M.; Davis, J. C. *At. Data Nucl. Data Tables* **1993**, *54*, 181. See also www-cxro.lbl.gov/optical_constants/.

(24) Regan, T. J.; Ohldag, H.; Stamm, C.; Nolting, F.; Lüning, J.; Stöhr, J.; White, R. L. *Phys. Rev. B* **2001**, *64*, 214422.

(25) Powell, C. J.; Jablonski, A. *NIST electron effective-attenuation-length database* (*SRD 71*), Version 1.1; National Institute of Standards and Technology: Gaithersburg, MD, 2001.

(26) Michaud, M.; Sanche, L. *Phys. Rev. A* **1987**, *36*, 4672.

(27) Odelius, M.; Cavalleri, M.; Nilsson, A.; Pettersson, L. G. M. Submitted for publication.

(28) Wilson, K. R.; Schuller, R. D.; Co, D. T.; Saykally, R. J.; Rude, B. S.; Catalano, T.; Bozek, J. D. *J. Chem. Phys.* **2002**, *117*, 7738.

(29) Timneanu, N.; Caleman, C.; Hajdu, J.; van der Spoel, D. *Chem. Phys.* **2004**, *299*, 277.

(30) Nilsson, A.; Wernet, Ph.; Nordlund, D.; Bergmann, U.; Cavalleri, M.; Odelius, M.; Ogasawara, H.; Näslund, L.-Å.; Hirsch, T. K.; Ojamäe, L.; Glatzel, P.; Pettersson, L. G. M. *Suppl. Mater. Sci.* **2005**, *308*, 793.

(31) The convolution algorithm is derived from an article by P. Marchand and L. Marmet (*Rev. Sci. Instrum.* **1983**, *54*, 1034) and is implemented in the WaveMetrics, Inc. software Igor version 4.04.

(32) Raghavan, K.; Foster, K.; Motakabbir, K.; Berkowitz, M. *J. Chem. Phys.* **1991**, *94*, 2110.

(33) Zhang, L.; Davis, H. T.; Kroll, D. M.; White, H. S. *J. Phys. Chem.* **1995**, *99*, 2878.

(34) Baker, J. M.; Dore, J. C.; Seddon, J. M.; Soper, A. K. *Chem. Phys. Lett.* **1996**, *256*, 649.

(35) Bellissent-Funel, M.-C. *J. Mol. Liq.* **1998**, *78*, 19.

(36) Cheng, L.; Fenter, P.; Nagy, K. L.; Schleger, M. L.; Sturchio, N. C. *Phys. Rev. Lett.* **2001**, *87*, 156103-1.

(37) Reedijk, M. F.; Arsic, J.; Hollander, F. F. A.; de Vries, S. A.; Vlieg, E. *Phys. Rev. Lett.* **2003**, *90*, 066103-1.

(38) Näslund, L.-Å. Probing unoccupied electronic states in aqueous solutions, Doctoral Thesis, Stockholm University, 2004, ISBN 91-7265-974.2. Available at http://www.diva-portal.org/su/theses/abstract.xsql?dbid=294

(39) Wernet, Ph.; Nordlund, D.; Bergmann, U.; Cavalleri, M.; Odelius, M.; Ogasawara, H.; Näslund, L.-Å.; Hirsch, T. K.; Ojamäe, L.; Glatzel, P.; Pettersson, L. G. M.; Nilsson, A. *Suppl. Mater. Sci.* **2004**, *304*, 995.